ENGINEER - Vol. LV, No. 01, pp. [13-21], 2022

DOI: http://doi.org/10.4038/engineer.v55i1.7482

Restrained Shrinkage of High Performance Concrete Comprising Silica Fume and Fly Ash

M. Rekatheeban and H.D. Yapa

Abstract: High performance concrete (HPC) is stronger/more durable than conventional concrete and its popularity has been widespread over the recent past. The composition of HPC is unique, for instance, it comprises high paste/aggregate volume, supplementary cementitious materials, etc. Consequently, some HPC characteristics are distinguished to be stern and one of those is shrinkage. For instance, HPC structures that are subjected to restrained conditions could experience undesirable non-structural cracking. In this context, this study assessed the restrained shrinkage behaviour of five HPC mixes conforming to the ASTM C1581 procedure. The mixes were designed for 50 MPa target cylinder compressive strength and comprised supplementary cementitious materials (SCMs) of 0-10% silica fume (SF) and 0-30% fly ash (FA). The results showed that the control and 10%SF/30%FA mixes had comparatively lower cracking potential under restrained conditions whereas the highest cracking potential was with the 10%SF/0%FA and 10%SF/10%FA mixes. Hence, shrinkage exaggerated with the addition of SF whereas that undesirability was compensated with the addition of FA. Meanwhile, the compressive strength of the control mix was enhanced approximately by 48% with the inclusion of 10%SF whilst the FA inclusion to the 10%SF mix reduced the compressive strength fairly proportional to the FA content. Overall, the strength varied in the range of 49 – 73 MPa. Mix 10%SF/20%FA had 26.5% higher compressive strength than the control mix and showed low risk on restrained shrinkage cracking. Hence, it was identified as a promising HPC combination. Similarly, 10%SF/30FA mix showed similar strength and crack potential characteristics to the control mix. That mix was accordingly identified as an ideal sustainable concrete mix for high-strength concrete applications.

Keywords: Cracking, Fly ash, Ring test, Silica fume, Shrinkage

1. Introduction

Concrete has been a leading construction material for decades owing to its attributes of appreciable strength, stiffness, durability, cost, fire performance, etc. In the recent past, a new concrete generation called high performance concrete (HPC) has become an attractive application particularly for large-scale construction [1,2]. HPC has special characteristics of high strength, high workability, high durability and low-permeability [1,2]. The use of supplementary cementitious materials (SCMs) is essential for HPC production [1]. Two such common SCMs are silica fume (SF) and fly ash (FA).

Time dependent non-structural deformation is a negative aspect inherent to concrete where shrinkage is a major course for such deformation. Shrinkage of concrete is primarily two-fold, autogenous shrinkage and drying shrinkage [1,3]. The higher the concrete strength, the larger is the autogenous shrinkage whereas vice-versa is true for drying shrinkage. In high strength concrete, low w/c ratios together with low water content are utilised. It is therefore reasonable to expect comparatively high autogenous shrinkage and comparatively low drying shrinkage in such concrete in contrast to normal strength concrete. These tendencies in shrinkage are comprehended only for OPC concrete. There is no guarantee that similar behaviour would prevail in the presence of SCMs. Hence, numerous research gaps exist about shrinkage of HPC.

Bamforth [4] reports that the use of SF increases concrete shrinkage. Since SF is an extra fine material, its use significantly refines the pore distribution in the cement paste [5]. It can therefore be anticipated that finer is the pore water distribution higher is the shrinkage. Meanwhile, Bamforth [4] showed that the addition of FA and ground granulated blast-furnace slag (GGBS) to concrete mitigates shrinkage [4].

Eng. M. Rekatheeban, B.Sc. Eng. (Hons)(Peradeniya), Department of Civil Engineering, University of Peradeniya.
E-mail:mtheeban1991@gmail.com
http://orcid.org/0000-0003-4230-1576
Eng. (Dr.) H. D. Yapa, AMIE (Sri Lanka), B.Sc. Eng. (Hons) (Moratuwa), Ph.D. (Cantab), Senior Lecturer of Civil Engineering, Department of Civil Engineering, University of Peradeniya.
E-mail:hdy@pdn.ac.lk
http://orcid.org/0000-0002-7213-5276

Qizhe [6] also experimentally proved that increasing fly ash content resulted in reduced concrete shrinkage. He further highlighted that a 30% fly ash replacement reduced both autogenous shrinkage and drying shrinkage by about 20%. Moreover, Mokarem et al. [7] compared the shrinkage predictions of several analytical models established for SCM based concrete and highlighted that the outcomes were highly inconsistent. Thus, comprehension of the shrinkage behaviour of SCM based concrete (and hence for HPC) is identified to be a challenge.

Concrete shrinkage is not significant if the concrete is free to move whereas it is serious when structural movements are fully/partially restrained. In the latter case, tensile stresses are generated which could result in undesirable cracking. The restraint can be external (because of end restraints) or internal (because of embedded reinforcement) [4]. Shrinkage associated cracking is a major concern for restrained flat concrete elements/structures (e.g. slabs) that are with a large exposed surface area to volume (A/V) ratio [2]. Typical examples are industrial floors, concrete pavements and bridge decks. Restrained shrinkage cracks, as opposed to flexural cracks, are parallel sided, and for slabs, usually extend right through the slab thickness. Such cracking may reduce both strength and durability [8]. Therefore, control of restrained shrinkage cracking is utterly important, and for that, accurate judgment of the shrinkage is vital.

The potential for shrinkage cracking of a concrete structure is influenced not only by the amount of shrinkage but also by the type of structure, degree of restraint, rate of strength/stiffness development, construction and curing methods, environmental conditions, etc. [9]. Several restrained shrinkage test configurations can be used to evaluate the cracking potential of concrete such as linear specimen tests and ring tests. Amongst them, the ring test is a popular and simple method which can be used to determine the relative effects of material variations on induced tensile stresses and cracking potential [2,9,10].

As previously mentioned, shrinkage prediction of HPC is a challenge but essential in terms of (restrained) crack control. Since SF is a crucial constituent for HPC and it apparently has negative impacts on shrinkage, it is deemed that exploration into restrained shrinkage behaviour of HPC is vital. Generally, 5% to 15% of SF can effectively be utilised for HPC production [1]. Ray et al. [2] explored the restrained shrinkage behaviour of HPC mixes comprising 5% SF and found that the SF blending had a considerable manipulation in this regard. However, such studies on the use of greater amount of SF are seldom found in the literature. Based on these observations, the current study was formulated to investigate the restrained shrinkage behaviour of HPC supplemented with 10% SF and 0 – 30% FA. A target cylinder compressive strength of 50 MPa was maintained.

2. Restrained Shrinkage Assessment: Ring Test

The ring test method is found in ASTM C1581 [9] and AASHTO PP 34-99 [10]. The test consists of a steel ring that acts as the restraining support for the concrete which is poured around, see Figure 1. The steel ring is equipped with two strain gauges placed horizontally at the ring mid-height and linked to a data recording system so that the strain in the steel ring is recorded every 30 minutes. Data recording is started immediately after casting of the specimen. Also, the specimen is inspected visually for cracking at time intervals not greater than three days. With the data recorded, ring strain with time can be plotted (see Figure 2), and the onset of concrete cracking can be identified from the point where the strain drops drastically.

Based on the availability of laboratory resources, the current study was conducted using the ASTM C1581 method. It indicates the potential of cracking based on two outputs, viz., (a) the time to first cracking (beyond the initiation of drying) and (b) the stress rate at cracking. As previously mentioned, the former (time) is identified directly from the graph and the latter (stress rate) is calculated as follows (further details are found elsewhere [9, 12]).

The net strain (ε_{net}) against the square root of elapsed time (t) for each strain reading is plotted, and linear regression analysis is performed to identify strain rate factor α from,

$$\varepsilon_{net} = \alpha\sqrt{t} + k \qquad \ldots(1)$$

where, k is a regression constant.

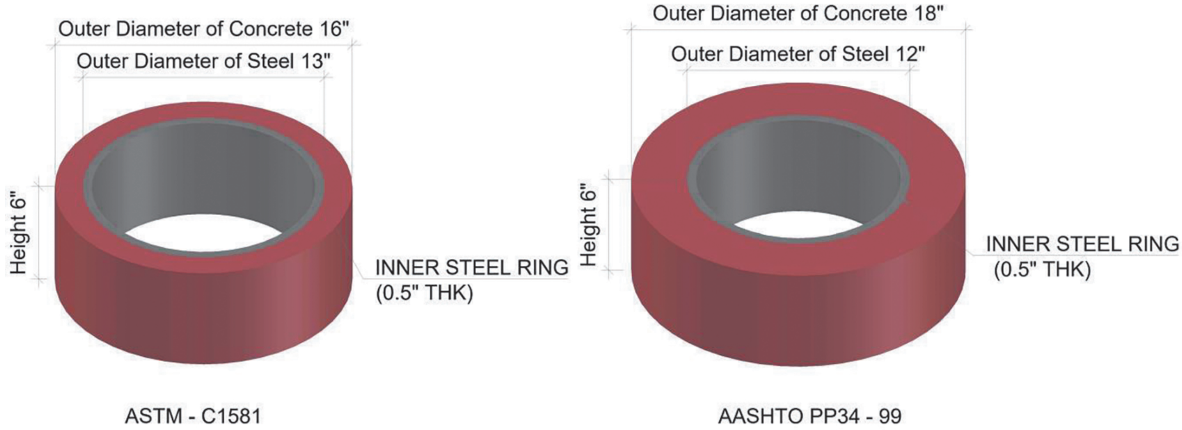

Figure 1 – ASTM and AASHTO Ring Test Detailing

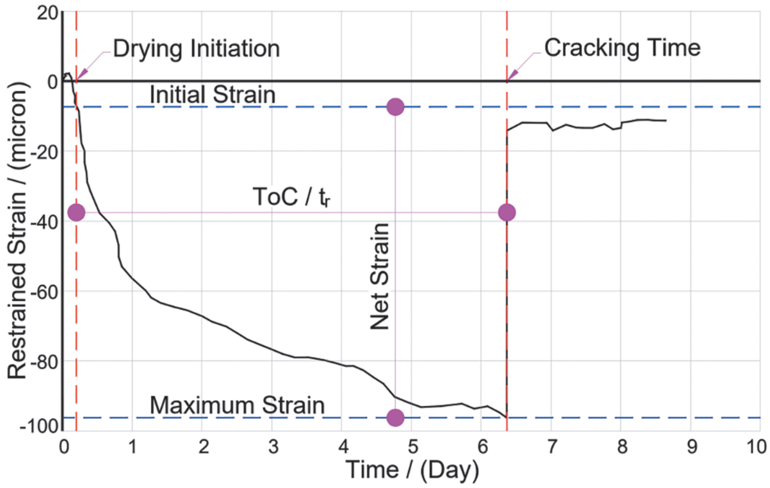

Figure 2 – Typical Strain vs. Time Behaviour in a Ring Test (ASTM C1581)

Average strain rate factor α_{avg} is found as the average α for the both strain readings for a ring specimen, and the stress rate at cracking (q) is defined as,

$$q = \frac{G|\alpha_{avg}|}{2\sqrt{t_r}} \qquad \ldots(2)$$

where G is a constant based on the ring dimensions (= 72.2 GPa for the ASTM C1581 test) and t_r is the elapsed time at cracking.

Based on the information on time to crack and stress rate at cracking, ASTM C1581 classifies the cracking potential of concrete as shown in Table 1.

Table 1 - Cracking Potential Classification (ASTM C1581)

Time-to-cracking, t_r, (day)	Stress rate at cracking, q, (MPa day^{-1})	Potential for cracking
$0 < t_r \leq 7$	$S \geq 0.34$	High
$7 < t_r \leq 14$	$0.17 < S < 0.34$	Moderate-High
$14 < t_r \leq 28$	$0.10 < S < 0.17$	Moderate-Low
$t_r > 28$	$S < 0.10$	Low

3. Experimental Procedure

An experimental study was carried out to explore the influence of the use of silica fume and fly ash on the restrained shrinkage behaviour of HPC via the ASTM C1581 ring test. The experimental series comprised five mix combinations including a control mix. Also, for each mix, two ring specimens and three 150 mm diameter 300 mm high cylinder specimens were cast. The target (cylinder) compressive strength for the control mix was

50 MPa (for a characteristic strength of 42 MPa) and the target workability was 400-600 mm slump-flow. For the SCM blended mixes, the SF level was kept constant at 10% cement replacement level while FA was blended at 0% to 30% variations.

3.1 Material Selection

Ordinary Portland cement (CEM 42.5N) was used as the main binder. Through trial mix designs, coarse aggregate passing 14 mm and retained on 10 mm sieves was identified to be appropriate to achieve the desired high strength level. The specific gravities of the coarse and fine aggregates were 2.76 and 2.60, respectively, and for SF and FA, were 2.30 and 2.45, respectively. In addition, AIV of the coarse aggregate and the fineness modulus of the fine aggregate were found to be 17.4 and 2.72, respectively. A superplasticizer based on polycarboxylic ether was used as an admixture.

3.2 Mix Proportioning

Mix design for the concrete was performed fixing the w/c ratio at 0.3. For the blended mixes, the binder proportions were computed considering the k-value concept introduced in EN 206-1 [11]. Based on the findings of Sanjeewa et al. [13], $k_{SF} = 2.0$ and $k_{FA} = 0.4$ were assigned in the concept. Table 2 shows the mix proportions for all the mixes. A notation is introduced in the table where the digits indicate the percentage of SCMs in the mix for SF and FA, respectively. For instance, 10SF/20FA denotes a mix of 10% SF, 20%FA and 70%OPC by weight.

3.3 Instrumentation and Specimen Casting

Two 10 mm gauge length strain gauges were fixed at the mid-height of the inner steel ring inner surface, see Figure 3. Concrete was poured into the ring mould and subsequently the setup was covered with a plastic sheet to prevent moisture loss. The strain readings in the steel rings were monitored using a computer-controlled data recording system which was programmed to store readings at 30 minute intervals. After 24 hours of cast, the cover was removed and the outer ring of the mould was demoulded. The top portion of each ring specimen was then wax coated to limit moisture loss only to the radial direction. A set of cast specimens are shown in Figure 4.

4. Results and Discussion

The following results were obtained from the experiment.

4.1 Fresh and Hardened Concrete Properties

A summary of the average cylinder strength and the slump flow of all the concrete mixes are presented in Table 2. It is observed that the addition of 10% SF to the control mix increased the compressive strength considerably (by ≈ 48%) whilst the inclusion of FA to the concrete mix comprising SF reduced the strength. The compressive strength of mix 10SF/30FA had a fairly similar strength to that of the control. Since the mix design was formulated according to the EN 206-1 k-value concept, these trends show that SF was more effective and FA was less effective than what was anticipated by the k-value concept (otherwise similar strengths should have been achieved). Meanwhile, the addition of SF to the control mix considerably reduced the workability of the control mix, whereas the inclusion of FA to the OPC/SF blend improved the loss of workability fairly proportional to the FA content (see Table 2). The 10SF/30FA mix exhibited similar workability to that in the control mix (it also possessed similar strength of the control mix). This particular combination can therefore be deemed to be a recommendable sustainable combination that can be used to produce concrete in the 50 MPa compressive strength range.

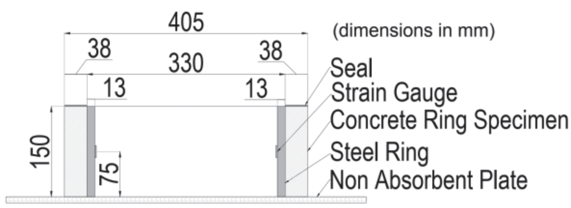

Figure 3 – Ring Test Arrangement

Table 2 – Mix Proportions

Mix	Mix proportion (kg/m^3)							Exp. results	
	Water	Cement	C. Agg.	F. Agg	Fly Ash (FA)	Silica Fume (SF)	Admix. (l)	Avg. Cylinder Strength (MPa)	Slump Flow (mm)
00SF/00FA	160	533	896	826	0	0	8.0	49	700
10SF/00FA	160	444	896	846	0	49	7.4	73	460
10SF/10FA	160	430	896	792	53	54	8.0	68	540
10SF/20FA	160	416	896	724	119	60	8.9	62	600
10SF/30FA	160	404	896	633	202	68	10.1	52	700

Figure 4 – Experimental Ring Test Specimens

4.2 Restrained Shrinkage Behaviour

All the ring specimens showed signs of cracking due to shrinkage. Figure 5 shows the cracking in two selected specimens.

Figure 5 - Restrained Shrinkage Cracking

Figures 6 (a) – (e) depict the strain measurements for the pair of rings for each mix. It is interesting to note that the ring pairs behaved fairly similarly in each context. These illustrations indicate the onset of first cracking with a large drop in the strain. It is of note that cracking was also observed visually in the specimens during the same time.

To compare the restrained shrinkage behaviours, the average of the strain readings are plotted in Figure 7. It is identified accordingly that mix 10SF/10FA exhibited the highest level of strain amongst the mixes. However, as previously mentioned, according to the behaviours of SF and FA, one would expect mix 10SF/0FA to be more shrinkage critical than mix 10SF/10FA but Figure 7 shows a slight contradiction. It is in fact, as guided in ASTM C1581, the cracking potential is not directly correlated to the level of strain (but to time to cracking and stress rate at cracking), and therefore further interpretation of the results is needed to draw conclusions.

Figure 8 illustrates the average time to crack for the experiments. It is of note that the time to crack was computed assuming drying started soon after the termination of curing (i.e., after 24 hrs.). It is highlighted that the control mix had the longest time to crack whereas the 10SF/00F mix exhibited the shortest time to crack. In that light, mix 10SF/00F had the highest potential for cracking. It is also noted that, as expected, the fly ash addition gradually delayed the crack onset.

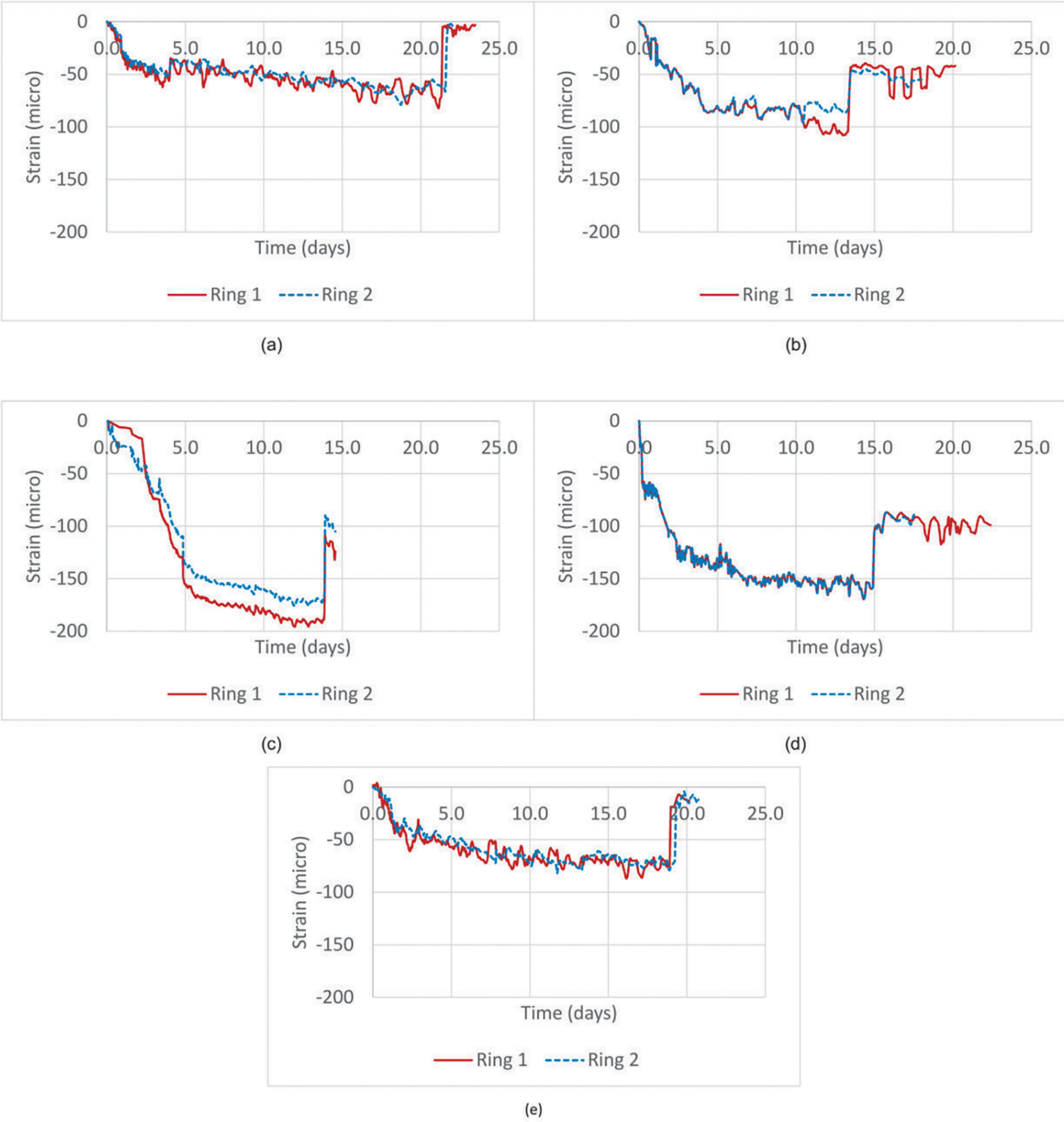

Figure 6 – Strain Development with Time Inside the Steel Ring: (a) 00SF/00FA; (b) 10SF/00FA (c) 10SF/10FA; (d) 10SF/20FA; (e) 10SF/30FA

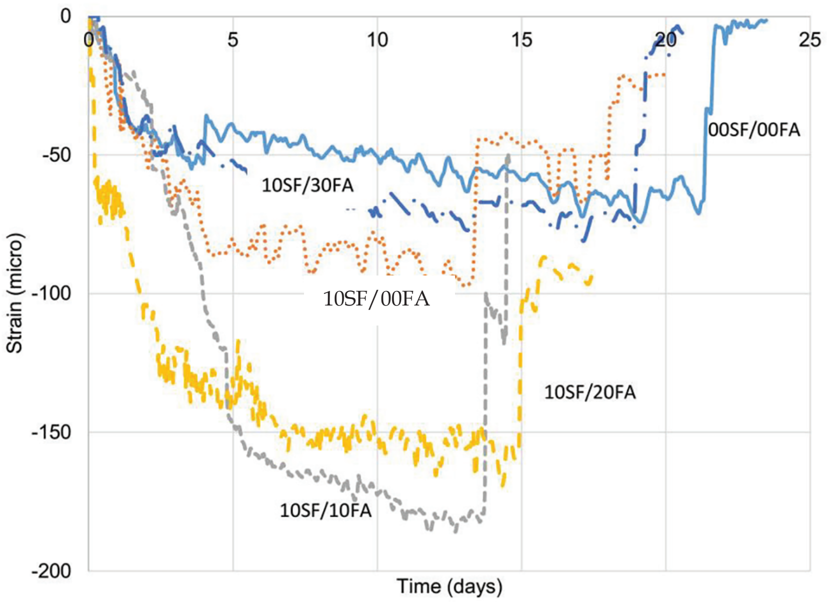

Figure 7 – Average Strain Development inside the Steel Ring

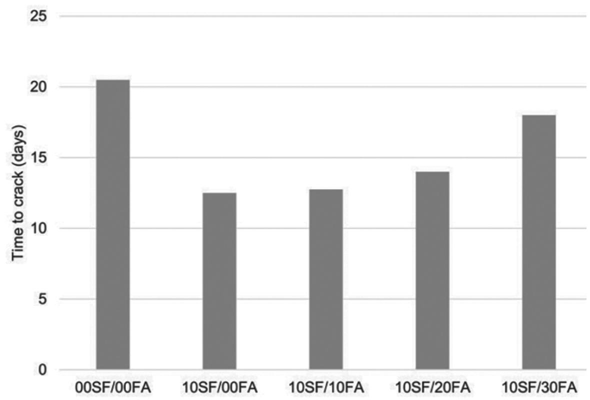

Figure 8 - Time to Crack of the Ring Test Specimens

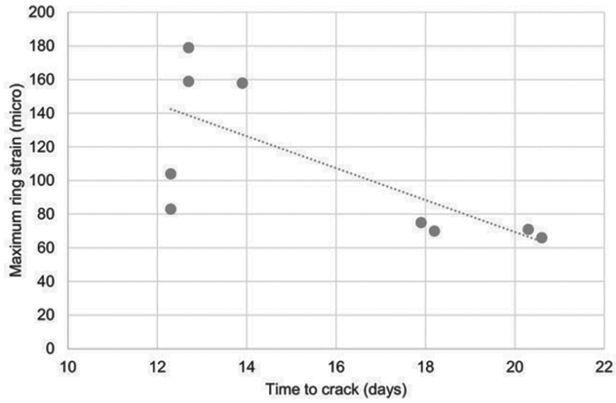

Figure 9 - Cracking Strain vs. Time to Crac

Figure 9 plots the maximum strain against the time to crack recorded for the mixes. It shows that, in general, higher the shrinkage quicker is to cracking, but as discussed in the preceding section, there is no direct correlation in-between. Interestingly, Hu et al. [14] also observed a similar behaviour in their ring test experimental series. In fact, the crack onset is not only in association with the shrinkage strain but also with other engineering properties of the concrete (e.g. strength, stiffness).

The average stress rate for the ring experiments was calculated based on the cracking condition of the ring test specimens via Eqns. 1-2. Table 3 presents the computed values. It also shows time to the onset of cracking and the cracking potential pertaining to each indication conforming to ATSM C1581.

The crack indications demonstrated in Table 3 highlight that the control and 10SF/30FA mixes had comparatively lower potential for cracking under restrained conditions. In terms of time to crack, the highest potential to crack was indicated in 10SF/00FA and 10SF/10FA mixes, whereas in terms of average stress rate, 10SF/10FA mix indicated the highest cracking potential. Hence, it is fair to state that both 10SF/00FA and 10SF/10FA mixes had a higher cracking potential at restrained conditions than the other mixes. Thus the inclusion of 10% of SF had detrimentally influenced the restrained shrinkage behaviour of concrete whilst the blending of 20% or more FA into the mix could control the risk of restrained shrinkage cracking. In fact, mix 10SF/20FA had 26.5% higher compressive strength than the control mix. In this light, that particular mix had appreciable strength as well as low risk of restrained shrinkage cracking, and can therefore be identified as a promising HPC combination.

Table 3 – Time to Crack, Average Stress Rate and Cracking Potential

Mix designation	Indication 1: Time to crack		Indication 2: Ave. stress rate	
	Time to crack / (day)	Cracking potential	Ave. stress rate of all mixtures / (MPa day^{-1})	Cracking potential
00SF/00FA	20.50	Moderate low	0.06	Low
10SF/00FA	12.50	Moderate high	0.22	Moderate high
10SF/10FA	12.75	Moderate high	0.54	High
10SF/20FA	14.00	Moderate high	0.21	Moderate high
10SF/30FA	18.00	Moderate low	0.09	Low

6. Conclusions

This study assessed the restrained shrinkage behaviour of five high performance concrete (HPC) mixes conforming to the ASTM C1581 procedure. The mixes were designed for 50 MPa target cylinder compressive strength, and comprised of supplementary cementitious materials (SCMs) of 0-10% silica fume (SF) and 0-30% fly ash (FA). Based on the findings, the following conclusions can be drawn.

1. The control and 10%SF/30%FA mixes indicated comparatively lower cracking potential under restrained conditions than the other three SCM mixes. The highest cracking potential was identified for the 10%SF/0%FA and 10%SF/10%FA mixes. The addition of FA in excess of 20% to OPC/SF mixes was identified to be important in terms of reducing the risk of non-structural cracking.
2. The compressive strength of the control mix was enhanced considerably (by about 48%) with the inclusion of 10%SF. In contrast, the FA inclusion to the 10% SF mix reduced the compressive strength fairly proportional to the FA content. Overall, the strength varied in the range of 49 – 73 MPa.
3. Mix 10SF/20FA had 26.5% higher compressive strength than the control mix and showed low risk on restrained shrinkage cracking. Hence, it can be identified as a promising HPC combination.
4. Since the mix design was formulated according to the EN 206-1 k-value concept, the resulting compressive strengths highlighted that, at this compressive strength range (49 – 73 MPa), SF was more effective and FA was less effective than that was anticipated by EN 206-1.
5. For the explored compressive strength range, 10%SF/30FA mix showed similar characteristics to the control mix in terms of compressive strength and of potential for non-structural cracking, Hence, this particular mix is recommendable as a sustainable combination to replace high-strength OPC mixes.

Acknowledgements

The authors wish to acknowledge the assistance provided by the technical staff of the Structures Laboratory and the Materials Laboratory of the Faculty of Engineering, University of Peradeniya.

References

1. Neville, A. M., (2011) *Properties of Concrete*. 5th ed., Pearson Education Limited, England.
2. Ray, I., Gong, Z., Davalos, J. F., and Kar, A., (2012) "Shrinkage and Cracking Studies of High Performance Concrete for Bridge Decks." *Construction and Building Materials* 28(1): 244-254.
3. Sung, Y., Kwon, S., and Jung, S. H., (2012) ''Analysis Technique for Autogenous Shrinkage in High Performance Concrete with Mineral and Chemical Admixtures''. *Construction and Building Materials*, 34: 1-10.
4. Bamforth, P. B., (2007) *CIRIA C660 Early-Age Thermal Crack Control in Concrete*, CIRIA, London, UK.
5. Lura, A., Breugel, K. V., and Maruyama, I. (2001) ''Effect of Curing Temperature and Type of Cement on Early-Age Shrinkage of High-Performance Concrete''. *Cement and Concrete Research* 31(12): 1867-1872.
6. Qizhe, H. (2013) *Setting behaviour and shrinkage of high performance pavement concrete: Effect of supplementary cementitious materials, chemical admixtures and temperature*. M.S. thesis, Department of Civil Construction and Environmental Engineering, Low a State University.
7. Mokarem, D. W, Weyers, R. E. and Lane, D. S. (2005) ''Development of a Shrinkage Performance Specifications and Prediction Model Analysis for Supplemental Cementitious Material Concrete Mixtures''. *Cement and Concrete Research* 35(5): 918-925.
8. Wei, D., Xiangming, Z., Zhimin, W. and Gediminas, K. (2016) ''Effects of Specimen Size on Assessment of Shrinkage Cracking of Concrete via Elliptical Rings: Thin vs. thick''. *Computers and Structures*, 174: 66- 78.
9. ASTM (2004) C1581-04: *Standard Test Method for Determining Age at Cracking and Induced Tensile Stress Characteristics of Mortar and Concrete under Restrained Shrinkage*. ASTM International, West Conshohocken, PA, USA.
10. AASHTO (2005) PP 34-99: *Standard Practice for Estimating the Crack Tendency of Concrete*.

11. EN 206-1 (2000): *Concrete - Part 1: Specification, Performance, Production and Conformity. Brussels, CEN.*

12. Rakatheeban, M. (2019) *Shrinkage Behaviour in High Performance Concrete Supplemented with Silica Fume and Fly Ash*. MEng thesis, University of Peradeniya, Peradeniya, Sri Lanka.

13. Sanjeewa, R. M. D. M., Pathirana, P. S. K. and Yapa, H. D. (2017) ''Mix Design Aspects of High Performance Concrete Comprised of Silica Fume and Fly Ash''. *Engineer: Journal of the Institution of Engineers, Sri Lanka,* 50(4): 23–29.

14. Hu, X., Shi, Z., Shi, C. et al. (2017) ''Drying Shrinkage and Cracking Resistance of Concrete Made with Ternary Cementitious Components''. *Construction and Building Materials* 149: 406-415.

15. SLS (2012) EN 1992-1-1. *Eurocode 2 - Design of Concrete Structures - Part 1-1 : General Rules and Rules for Buildings*. SLSI, Colombo, Sri Lanka.

16. Gilbert, R. I., (2017) ''Cracking Caused by Early-Age Deformation of Concrete – Prediction and Control''. *Procedia Engineering* 172: 13-22.

17. Mosley, B., Bungey, J. and Hulse, R. (2012) *Reinforced concrete design to Eurocode 2.* 7th ed., Palgrave Macmillan, Hampshire, UK.

18. Nanayakkara, S. M. A., and Wannigama, W. R. K. (2003) ''Experimental Investigations on Temperature Rise due to Heat of Hydration''. *Annual transactions of Institution of Engineers*, Sri Lanka: 9-15.